

Full Length Research Paper

Photopyroelectric characteristics of Pr_6O_{11} – ZnO ceramic composites

Zahid Rizwan¹, M. G. M. Sabri¹ and B. Z. Azmi^{1,2*}

¹Department of Physics, Faculty of Science, Universiti Putra Malaysia, 43400 UPM Serdang, Selangor D.E., Malaysia.

²Advanced Material and Nanotechnology Laboratory, Institute of Advanced Technology, Universiti Putra Malaysia, 43400 UPM Serdang, Selangor D.E., Malaysia.

Accepted 04 January, 2011

Characteristics of different Pr_6O_{11} ceramic composites were studied using photopyroelectric spectroscopy. The amount of Pr_6O_{11} in the composite was varied from 0.1 to 0.75 mol% at the sintering temperature of 1190 and 1270°C. It was found that optical energy band-gap (E_g) of the composite is reduced by increasing the amount of Pr_6O_{11} in the composite at both sintering temperatures. However, the decrease in E_g was relatively less at a sintering temperature of 1270°C as compared to that of 1190°C. XRD analysis showed that all samples have two phases, that is ZnO and intergranular layers composed of Pr_6O_{11} and few small peaks of Pr_2O_3 . EDAX results further showed that the Pr_6O_{11} and Pr_2O_3 were segregated in the grain boundaries. Maximum grain size of 5.85 μm and relative density of 94.5% were found in these ceramics at $x = 0.1$ and 0.5 mol%, respectively, for 1270°C sintering temperature.

Key words: Photopyroelectric spectroscopy, optical energy band gap, Pr_6O_{11} , ZnO.

INTRODUCTION

White color polycrystalline Zinc oxide (ZnO) is a versatile and important semiconductor which has attracted significant attraction because of its characteristic properties like transparency in visible spectrum, direct band gap, absence of toxicity, abundance in nature, etc. These properties find wide technological applications (Look, 2001). It is used in batteries, electrical components such as piezoelectric transducers, phosphors, blue laser diodes and varistors (Hevia, 2005). Varistors exhibit high nonlinear current-voltage characteristics (Clarke, 1999). So they are used to protect semiconductor devices, circuits and power systems from dangerous over voltages.

Varistor effect which can be explained on the basis of the double Schottky-type potential barriers associated with defects in the vicinity of grain boundaries (Ammar and Farag, 2010; Feng et al., 2010; Cardaro and Shim,

1986; Friedrich and Arefin, 2010). Many varistor forming oxides (VFO) like BaO, Bi_2O_3 , Pr_6O_{11} , V_2O_5 , and La_2O_3 are being used to fabricate ZnO based varistors. Their chemical properties and structures are markedly different. All of them exhibit fixed oxidation state except Pr_6O_{11} . The commercial varistors necessarily contain Bi_2O_3 as varistor-forming oxides (VFO) and show excellent varistor properties. Bi_2O_3 containing varistors have some drawbacks like high volatility and reactivity as Bi_2O_3 melts during the sintering above 1000°C. High volatility changes the varistor characteristics with the variation of inter composition ratio of additives. High reactivity of Bi_2O_3 destroys the multilayer structure of chip varistor. It generates many secondary phases which destroy the surge absorption capabilities of the varistor. It has been studied ZnO based varistor containing Pr_6O_{11} as a VFO to overcome the problems.

The exact role of dopants in the electronic structure of ZnO varistor is still uncertain. These dopants are the main tools that are used to improve the non-linear characteristics and the stability of the ZnO based varistor

*Corresponding author. E-mail: azmizak@gmail.com.

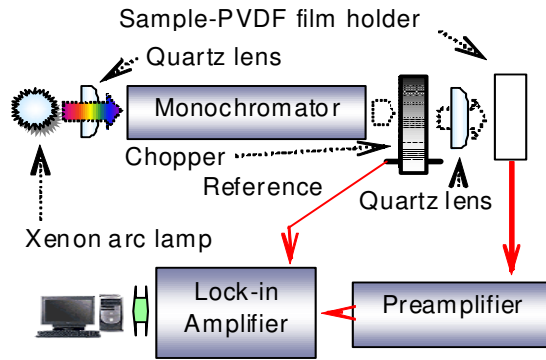


Figure 1. Schematic diagram of experimental setup.

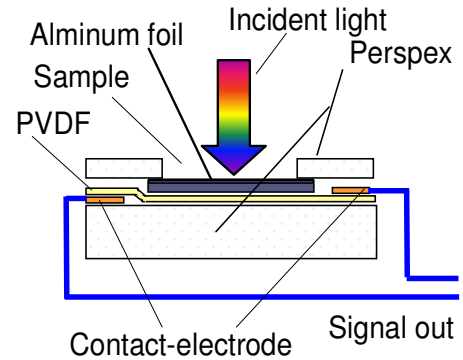


Figure 2. Schematic diagram of homemade PVDF sensor holder.

(Eda, 1989). So it is necessary to get information of optical absorption behavior for the investigation of the electronic states in this ceramic combination. A powerful non-radiative investigation photopyroelectric (PPE) spectroscopy is used to study the optical absorption behavior for such ceramic combination (Minamide et al., 1998).

The main objective of this study is to investigate the optical absorption behavior of $x\text{Pr}_6\text{O}_{11}$ doped ZnO ceramic at different sintering temperatures. This investigation is necessary to have a good knowledge of optical absorption in order to understand the electronic structure of the Pr_6O_{11} doped ZnO.

MATERIALS AND METHODS

ZnO (4N purity, Alfa Aesar) was doped with $x\text{Pr}_6\text{O}_{11}$ (3N purity, Alfa Aesar), $x = 0.1, 0.25, 0.50$ and 0.75 mol%. Ball milled powder of each mole percent was pre-sintered at a temperature of 700°C for 120 min in an open atmosphere at the heating and cooling rate of $2.5^\circ\text{C min}^{-1}$. Polyvinyl alcohol (1.1 wt %) was mixed as a binder to avoid the cracks in the ceramic. Powder were pressed under a force of 780 kg cm^{-2} to form a disk of 10 mm diameter with about 1.2 mm thickness and then sintered at 1190 and 1270°C for 2 h in air. The disk from each sample was ground and sieved for the PPE spectroscopy and XRD analysis. The samples were thermally etched for the microstructure analysis. Cu K_α radiation with PANalytical (Philips) X'Pert Pro PW1830 was used for XRD analysis. The XRD data were analyzed by X'Pert High Score software for the identification of the crystalline phases.

Measurement of the PPE signal was made by PPE spectrometer as described elsewhere (Mandelis, 1984) (Figure 1). Disk of each sample was ground in doubly deionized water. Few drops from each mixture were dropped separately on an aluminum foil to form a thin film of the sample and dried at room temperature for PPE signal measurement. The Aluminum foil was placed in contact to a polyvinylidene difluoride (PVDF) PPE sensor using silver conductive grease in between two Perspex plates of homemade sample holder (Figure 2). A 1 kW Xenon arc lamp light beam in wavelength range from 300 to 800 nm was used in this measurement and its beam was mechanically modulated at frequency of 10 Hz. The optical absorption coefficient (β) varies with the incident photon energy ($h\nu$) and is given by the expression,

$(\beta h\nu)^2 = C(h\nu - E_g)$, C is constant and E_g is the optical energy band-gap.

PPE signal intensity (ρ) is directly proportional to β , hence $(\rho h\nu)^2$ is related to $h\nu$ linearly. E_g is obtained by extrapolating the linear fitted region from the plot of $(\rho h\nu)^2$ versus $h\nu$ (Toyoda et al., 1985; Ates et al., 2007; Hua et al., 2006; Kumara et al., 2009). An optical-absorption edge has been observed in a variety of amorphous and crystalline materials. The optical-absorption edge has important role in electron or exciton-phonon interactions (Toyoda et al., 1987). It is found that PPE signal intensities plotted semi logarithmically varies linearly with the photon energy ($h\nu$) just lower than the fundamental absorption edge (Urbach, 1953). An empirical relation for absolute measuring temperature (T) and photon energy ($h\nu$) is given by equation (1):

$$P = P_0 e^{\sigma(h\nu - h\nu_0)/kT} \quad (1)$$

Where k is the Boltzmann's constant and P_0 , σ , ν_0 are fitting parameters (Dow and Redfield, 1972; Qing and Toyoda, 1999). The value σ/kT , determines the exponential slope, where σ is the steepness factor and is characterized in optical absorption edge. The steepness factor is found (σ_A in region-A and σ_B in region-B) from the PPE spectrum.

RESULTS AND DISCUSSION

Microstructural features

XRD analysis of the ceramic ZnO doped with Pr_6O_{11} show that there are only two phases. The major phase is ZnO (ref. code 00-005-0664) and few small peaks of Pr_6O_{11} and Pr_2O_3 are present in the ceramics at both temperatures 1190 and 1270°C . Small peaks at an angle $2\theta = 28.1268^\circ, 46.4873^\circ$ for the planes (200) and (220) belong to cubic Pr_6O_{11} , respectively (ref. code 00-042-1121) at both sintering. These peaks are more prominent at 1270°C sintering temperature. Few peaks at an angle $2\theta = 30.035^\circ, 62.9309^\circ$ and 68.1916° for the planes (101), (202), (104) belong to hexagonal Pr_2O_3 , respectively, (ref. code 00-022-0880) at both sintering

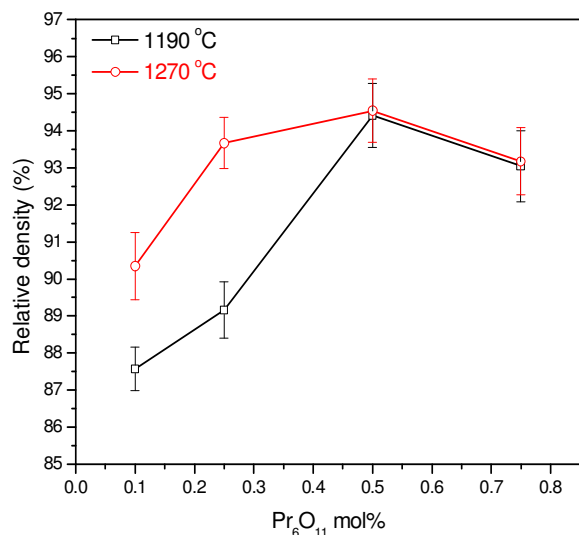


Figure 3. Variation of density with Pr₆O₁₁ doping level.

temperatures. These peaks are also clearer at 1270 °C sintering temperature for higher doping level of Pr₆O₁₁.

The relative density (Figure 3), increased from 87.6 to 94.5% with the increase of Pr₆O₁₁ and it becomes constant at about 0.5 mol% Pr₆O₁₁ which indicates the increase of Pr₆O₁₁ reduces the pores and enhances the densification mechanism. The density of the ceramics has higher values at the higher sintering temperature 1270 °C. This indicates the densification process is more enhanced with the increase of sintering temperature. The microstructure is quite uniform through the samples at both sintering temperatures. The abnormal grain growth is not also observed for all the samples (Figure 4). The average grain sizes obtained by the linear intercept method on different locations were reproducible. The grain size is reduced slightly from 2.6 to 1.6 μm with the increases of Pr₆O₁₁ at 1190 °C sintering temperature (Figure 5). This indicates the Pr₆O₁₁ reduces the grain size slightly. The grain size of the ceramic is 5.8 μm at 0.1 mol% of Pr₆O₁₁ and is reduced with the increase of doping level. Its value is reduced to 3.7 μm at 0.75 mol% of Pr₆O₁₁ at 1270 °C sintering temperature. The white clusters of Pr rich phase are confirmed by EDX. Pr₆O₁₁ and Pr₂O₃, are segregated in the grain boundaries as well as at the triple point junctions.

The continuous distribution of the Pr-rich intergranular material observed in the samples soaked at higher temperature. White spots are clear at the higher doping level of Pr₆O₁₁. The segregation is more at the higher doping level and at the higher sintering temperature.

Optical features

The energy band-gap (E_g) of the ceramics ZnO

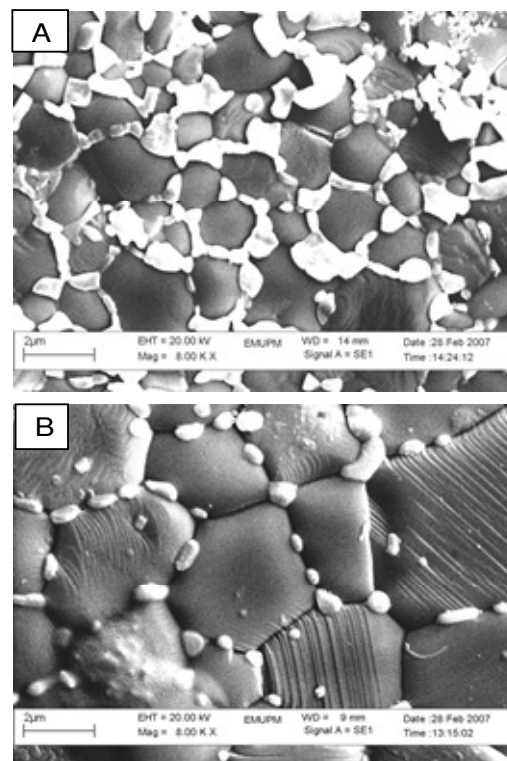


Figure 4. SEM micrograph at sintering temperature (A) 1190 °C, (B) 1270 °C and doping level (A) 0.75 mol% Pr₆O₁₁, (B) 0.1 mol% Pr₆O₁₁.

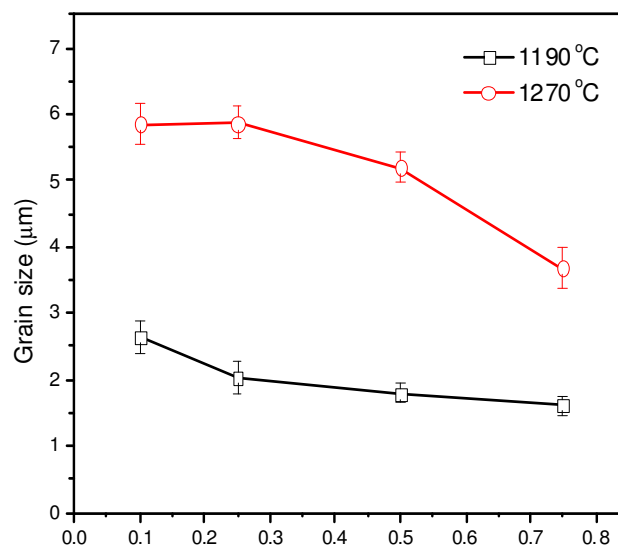


Figure 5. Variation of grain size with Pr₆O₁₁ doping level.

decreases from 3.2 (pure ZnO) to 2.90 ± 0.01 eV at 0.1 mol% Pr₆O₁₁ at 1190 °C for 2 h sintering time (Figure 6). This decrease is 0.3 eV at 0.1 mol% doping level of Pr₆O₁₁ and is due to the growth of interface states at the

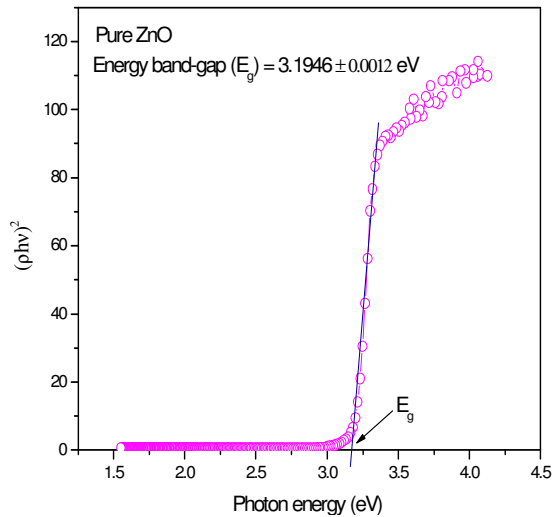


Figure 6. Energy band gap of pure ZnO.

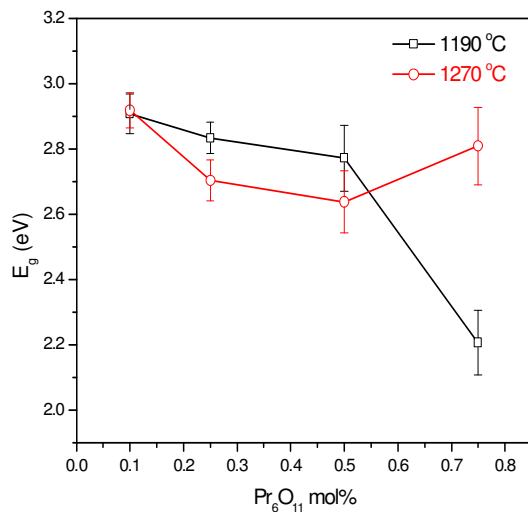


Figure 7. Variation of E_g with Pr_6O_{11} doping level.

grain surface as well as grain boundaries (Figure 7). The value of E_g decreased to 2.20 ± 0.01 eV with the increase of Pr_6O_{11} at 0.75 mol% Pr_6O_{11} . This decrease, 0.7 eV, is due to the growth of interface states due to Pr ions at the grain boundaries and at the grain surfaces. The value of E_g of the ceramics ZnO decreases from 3.2 to 2.91 ± 0.01 eV at 0.1 mol% of Pr_6O_{11} for 2 h sintering time at the sintering temperature of 1270 °C. This decrease is due to the 0.1 mol% doping level of Pr_6O_{11} .

The value of E_g further decreased to 2.80 ± 0.01 eV up to 0.5 mol% of Pr_6O_{11} . This slight decrease, 0.11 eV, in the value of E_g is due to the growth of interface states at the particle surfaces and at the grain boundaries as Pr rich phases are segregated at the grain boundaries as

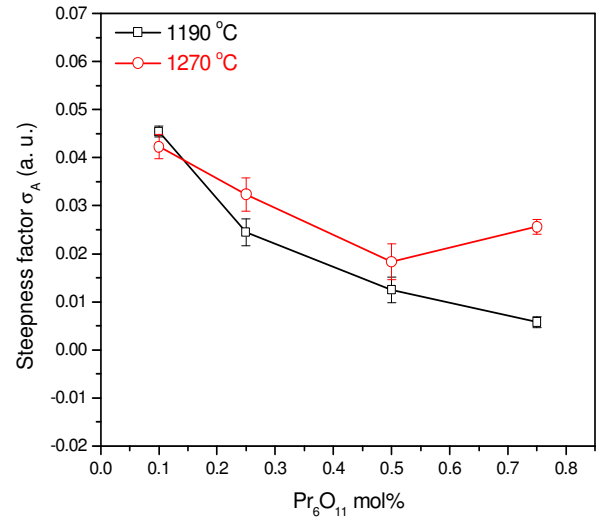


Figure 8. Effect of Pr_6O_{11} doping on steepness factor σ_A .

shown in Figure 7. But at 0.75 mol% Pr_6O_{11} , the growth of interface states is reduced and the value of E_g slightly increases. This is due to the decrease in the interface states and may be due to the segregation, especially in the grain boundaries as Pr rich phases Pr_2O_3 or Pr_6O_{11} are segregated in the grain boundaries or due to the secondary phases which are below the detection limit. The steepness factor σ_A (Figure 8), decreases with the increase of Pr_6O_{11} mol% at both sintering temperature 1190 and 1270 °C. This indicates the increase in the PPE signal intensity which suggests that the structural ordering decreases with the increases of Pr_6O_{11} at 1190 and 1270 °C sintering temperature. So the growth of the interface states takes place at both sintering temperatures.

The value of E_g decreases with the increases of doping level showing the increase in the interface states, Figure 7. The value of the steepness factor σ_A increases at 0.75 mol% of Pr_6O_{11} and the value of E_g increases negligibly for the sintering temperature of 1270 °C and there is the same trend in steepness factor σ_A and in E_g for the sintering temperature 1270 °C. This may be due to the segregation of the Pr_6O_{11} in the grain boundaries or secondary phases at higher sintering temperature. Generally an exponential tail (in region-B) for crystalline semiconductors can be characterized by Equation (2),

$$(\sigma_B/KT)^{-1} = A \langle U^2 \rangle_T / C_0 \quad (2)$$

Where C_0 is the exponential tail parameter of the order of unity and $\langle U^2 \rangle_T$ is the thermal average of the square of the displacement of the atoms from their equilibrium positions. The term $\langle U^2 \rangle_T$ expresses the energy of displacement of atoms (Toyoda and Shimamoto, 1998; Toyoda et al., 1997; Tauc, 1981). The steepness factor, σ_B (region-B in PPE spectra), decreases with the

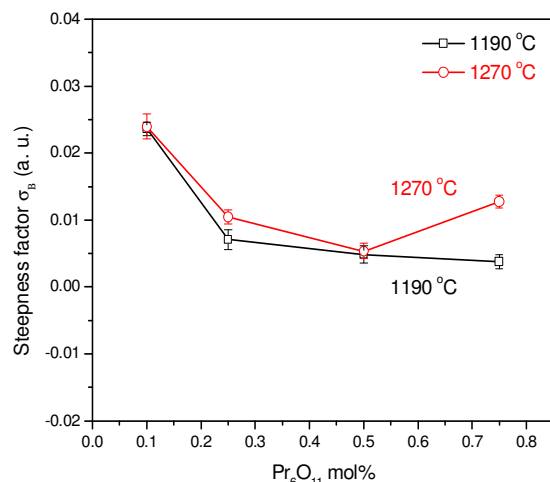


Figure 9. Effect of Pr₆O₁₁ doping on steepness factor σ_B .

increase of Pr₆O₁₁ mol% at 1190°C sintering temperature (Figure 9). This indicates that the increase in the average thermal energy of displacement of atoms at this sintering temperatures 1190°C. This suggests the structural disordering is increasing with the increase of the Pr₆O₁₁ doping level and resultantly the value of the E_g decreased (Figure 7).

The steepness factor, σ_B decreases with the increase of Pr₆O₁₁ mol% at 1270°C sintering temperature (Figure 9). This indicates that the increase in the average thermal energy of displacement of atoms at this sintering temperatures 1270°C. This suggests the structural disordering is increasing with the increase of the Pr₆O₁₁ doping level and resultantly the value of the E_g decreased (Figure 7). The trend in the variation of the value of σ_B is same as in the variation of E_g .

Conclusion

XRD results confirmed the hexagonal phase of ZnO and intergranular layers of Pr₆O₁₁ and few peaks of Pr₂O₃. EDAX analysis shows that the Pr₆O₁₁ is segregated in the grain boundaries and at the triple point junctions. Optical energy band-gap is reduced to 2.20 eV at higher doping level of Pr₆O₁₁ for 1190°C sintering temperature. PPE spectroscopy can be used successfully to study the optical absorption behavior along with the other electrical measurements of ZnO-based varistor.

ACKNOWLEDGEMENTS

The authors are thankful to the Malaysian Ministry of Higher Education for funding this research work through FRGS Project # 01-01-07-139FR.

REFERENCES

- Ammar AH, Farag AAM (2010). Investigation of deep level transient spectroscopy (DLTS) of dopant ZnO-based varistors, *Physica B.*, 405: 1518-1522.
- Ates AM, Yildirim A, Kundakci M, Yildirim M (2007). Investigation of optical and structural properties of CdS thin film. *Chin. J. Phys.*, 45(2-1): 135-141.
- Clarke DR (1999). Varistor ceramics. *J. Am. Ceram. Soc.*, 82(3): 485-502.
- Cardaro JF, Shim Y (1986). Bulk electron trap in Zinc oxide varistors. *J. Appl. Phys.*, 50(12): 4186-4190.
- Dow JD, Redfield D (1972). Towards a unified theory of Urbach's rule and exponential absorption edge. *Phys. Rev. B.*, 5: 594-610.
- Eda K (1989). Zinc Oxide varistors. *IEEE Elect. Insul. Mag.*, 5: 28-41.
- Feng H, Peng Z, Fu X, Fu Z, Wang C, Qi L, Miao H (2010). Effect of TiO₂ doping on microstructural and electrical properties of ZnO-Pr₆O₁₁-based varistor ceramics. *J. Alloy. Compd.*, 497: 304-307.
- Friedrich RM, Arefin L (2010). Kinetic field approach to study liquid phase sintering of ZnO based ceramics. *Ceram. Int.*, 36: 1429-1437.
- Hevia DF, Caballero AC, Frutos J, Fernandez JF (2005). Dominance of deep over shallow donors and the non-Debye response of ZnO-based varistors. *J. Eur. Ceram. Soc.*, 25: 3005-3009.
- Hua S, Leeb YYC, Shenc JL, Chenc KW, Tiongd KK, Huang YS (2006). Temperature dependence of absorption edge anisotropy in 2H-MoSe₂ layered semiconductor. *Solid State Commun.*, 139: 176-180.
- Kumara V, Sonkawadeb RG, Dhaliwala A, Mehrac SR (2009). Study of neutron induced modification on optical band gap of CR-39 polymer detector. *Asian J. Chem.*, 21(10): S279-283.
- Look DC (2001). Recent advances in ZnO materials and devices. *Mat. Sci. Eng. B-Solid*, 80: 383-387.
- Minamide AM, Shimaguchi Y, Tokunaga T (1998). Study on photopyroelectric signal of optically opaque material measured by PVD film sensor. *Jpn. J. Appl. Phys.*, 37: 3144-3147.
- Mandelis A (1984). Frequency-domain photopyroelectric spectroscopy of condensed phases (PPES): A new, simple and powerful spectroscopic technique. *Chem. Phys. Lett.*, 108: 388-392.
- Qing S, Toyoda T (1999). Photoacoustic studies of annealed CdSxSe1-x (x = 0.26) Nan crystals in a glass materials. *Jpn. J. Appl. Phys.*, 38: 3163-3167.
- Toyoda T, Nakanishi H, Endo S, Irie T (1985). Fundamental absorption edge in semiconductor CdInGaS₄ at high temperatures. *J. Phys. D Appl. Phys.*, 18: 747-751.
- Toyoda T, Nakanishi H, Endo S, Irie T (1987). Hydrostatics pressure dependence of the exponential optical absorption in CdInGaS₂. *J. Appl. Phys.*, 61(1): 434-436.
- Toyoda T, Fujimoto H, Konaka T (1997). Dependence of the photacoustic signal intensity spectra on sintering temperature for ceramic CdS_{0.5} and CdS_{0.5}Se. *Jpn. J. Appl. Phys.*, 36: 3292-3296.
- Toyoda T, Shimamoto S (1998). Effect of Bi₂O₃ in ceramic ZnO on photoacoustic spectra and current voltage characteristics. *Jpn. J. Appl. Phys.*, 37: 2827-2831.
- Tauc J(Ed) (1981). *Amorphous and Liquid Semiconductors*. Plenum Press London, p. 159.
- Urbach F (1953). The long wave length edge of photographic sensitivity and of the electronic absorption of solids. *Phys. Rev.*, 92: 1324.